Journal of Solid State Chemistry **162,** 364–370 (2001)
doi:10.1006/jssc.2001.9412, available online at http://www.idealibrary.com on IDEAL®

Direct Fabrication of Lithium Cobalt Oxide Films on Various Substrates in Flowing Aqueous Solutions at 150°C

Tomoaki Watanabe, Hiroyuki Uono, Seung-Wan Song, Kyoo-Seung Han, and Masahiro Yoshimura

Center for Materials Design, Materials and Structures Laboratory, Tokyo Institute of Technology, 4259 Nagatsuta, Midori, Yokohama 226-8503, Japan

IN HONOR OF PROFESSOR PAUL HAGENMULLER ON THE OCCASION OF HIS 80TH BIRTHDAY

In this paper, a newly developed idea for direct fabrication of double oxide films on various substrates, the "dual anode system," is described. Films of $LiCoO_2$ were directly fabricated on Pt, Ni, and graphite substrates by a hydrothermal–electrochemical method at 125–175°C for 2 hours in a flow cell using a cobalt metal anode as a cobalt ion source and a 4M LiOH aqueous solution as a lithium source, without any subsequent firing or annealing. The target substrate (Pt, Ni, or graphite) was also connected to the anode in the dual anode system. The addition of an oxidant, H_2O_2, in the flowing LiOH solution has produced $LiCoO_2$ films in a short reaction time of 2 h using the flow cell. The H_2O_2 seems to accelerate the oxidation of Co^{2+} into Co^{3+} in cobalt species during the reactions, dissolution–oxidation–precipitation. The thickness and the microstructure of the films could be controlled. In optimum conditions, the film consisting of plate-like $LiCoO_2$ crystals at most a few micrometers thick could be obtained. Micro-Raman and X-ray diffraction studies demonstrated that increasing the fabrication temperature produces a phase change in $LiCoO_2$ from spinel to hexagonal. Spinel phase $LiCoO_2$ is obtained around 125°C and hexagonal phase appears above 125°C. Above 150°C, the redissolution rate of formed crystals seems to dominate the formation of crystals; thus the grain size decreases with increasing temperature. © 2001 Elsevier Science

INTRODUCTION

Lithium transition metal double oxides with layered or spinel structures are efficient as cathode materials for lithium rechargeable batteries. Among these layered and spinel structure materials, $LiCoO_2$ compounds are regarded as the most promising because of their high energy density and high recycle ability (1–8). However, with increasing consumption demand on the battery, several problems have occurred. Nowadays, one of the most important problems in industry is the environmental impact of high energy consumption and/or toxic waste from fabrication processes (9, 10). In general, the production of cathode electrodes needs several complicated multistep procedures. For example, in $LiCoO_2$ film fabrication by classical solid-state reaction, the first step is the synthesis of the powder, then shape formation and last fixation on the substrate. They can also be fabricated directly by CVD or PVD, but these methods require more energy than conventional solid-state reaction (9). Since these methods not only need complicated procedure but also need high temperatures or high energies, it is difficult to regard them as environmentally friendly method. Compared to such physical methods, direct film formation from an aqueous solution is thought to be simpler and more economical and requires much less energy consumption (9, 10). From this point of view, our group has demonstrated the utility of soft solution processing (11–18), which is defined as environmentally friendly processing to fabricate a variety of functional solid materials in particular shapes, sizes, locations, etc., using (aqueous) solutions. Recently, we reported the successful fabrication of electrochemically active $LiMO_2$ (M = Ni, Co) films in a single synthetic step by electrochemical and/or hydrothermal methods without any firing or annealing (19–23). In addition, we have succeeded in producing a lithium cobalt oxide film even at room temperature (24). However, solution methods using hydrothermal–electrochemical reactions require particular conditions. For example, Co substrate is needed for $LiCoO_2$ films and Ni substrate for $LiNiO_2$.

In the present study, we have succeeded in fabricating $LiCoO_2$ films on various substrates (Pt, Ni, and graphite) for the first time by developing a "Dual Anode System". Formation and growth mechanism, phase and microstructural changes of $LiCoO_2$ films have also been studied.

EXPERIMENTAL PROCEDURE

(1) Flow Cell for Hydrothermal–Electrochemical Synthesis

All the experiments have been accomplished in the handmade flow cell for hydrothermal–electrochemical synthesis, which is schematically shown in Fig. 1. Details of the flow cell have been reported in our previous paper (25). Solution can be pumped from the container(s) to the flow cell at a flow rate of 0.1–50 ml/min. Our flow system can operate at up to 200°C, which is an adequate temperature even for

0022-4596/01 $35.00

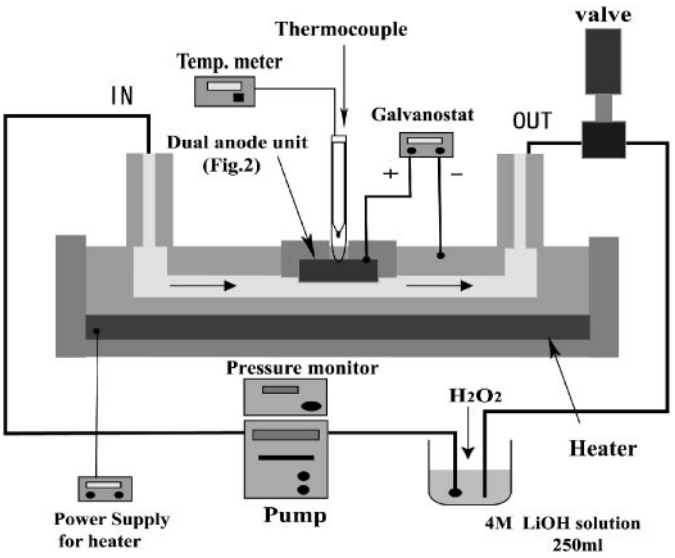

FIG. 1. Schematics of the flow cell system for hydrothermal–electrochemical reactions.

industrial applications of hydrothermal synthesis. The temperature is detected by a chromel–alumel thermocouple just below the substrate and controlled by changing the input power of the heater. Electrochemical conditions are controlled in a range determined by our potentiostat/galvanostat equipment (Kikusui Electronics Corp., Japan).

(2) Preparation of $LiCoO_2$ Thin Films

H_2O_2-added 4 M LiOH solution has been used in the flow cell with dual anode system in the fabrication of lithium cobalt oxide films on various substrates. Reagent grade $LiOH{\cdot}H_2O$ (Wako Pure Chemical Industries Ltd., Japan) and polished cobalt plate (purity 99.5%, Nilaco Corp., Japan) were used as sources of lithium and cobalt, respectively. The washed platinum, nickel, and graphite plates (Nilaco Corp., Japan) were used as a target substrate in the "dual anode system." The arrangement of the dual anode system in the flow cell is shown in Fig. 2. The cobalt plate is connected to the positive electrode (anode) and the body of flow sell connected to the negative electrode (cathode). The target substrate was also connected to anode with a Ti foil of 50 μm thickness as the spacer. In all experiments, galvanostatic conditions with constant current densities of 1 mA/cm^2 were applied. Appropriate quantities of LiOH were dissolved in distilled water to yield 4 M solutions. During the experiments, the 30% H_2O_2 solution was constantly added as an oxidant to the LiOH solution at 1 ml/h. Experiments have been carried out for 2 h at 125, 150, and 175°C. The circulation of the solution was assisted by a high-pressure pump with a flow rate of 5 ml/min under open flow. The pressure in the flow cell was kept at 2 MPa by a needle valve attached at the output pipe of the flow cell.

(3) Characterization

The crystals formed in the film structure were characterized by an X-ray diffractometer (Model MXP3VA, MAC Science Co., Tokyo) with Cu$K\alpha$ radiation at 40 kV and 40 mA. Surface morphologies of the films were observed using scanning electron microscope (SEM) (S-4500, Hitachi, Tokyo). Film thickness and film surface morphology were also examined using a field emission scanning electron microscope (Model S-4500, Hitachi, Tokyo). Raman scattering spectra excited with the 514.5-nm line of an Ar laser with power 5 mW were detected at room temperature. The laser beam was focused on a 1-μm diameter circle on the film surface with a microscopic objective lens. The scattered light was analyzed with a triple spectrometer (Model T64000, Jobin Yvon/Atago Bussan, Tokyo) and detected using a liquid-nitrogen-cooled CCD detector.

RESULTS AND DISCUSSION

As reported in our previous papers (20–23), $LiCoO_2$ films could be fabricated directly on a Co substrate by the hydrothermal–electrochemical method at 100–200°C for around 20 hours in LiOH solution. In the present study we combined two new techniques: one is the use of the flow cell to add oxidant (H_2O_2) constantly into the reactant solution and the other is the dual anode system for direct fabrication of $LiCoO_2$ films on various substrates. They make it possible to decrease reaction time down to 3 h for direct preparation of $LiCoO_2$ films and also to deposit the films directly on various substrates. The effect of the oxidant on

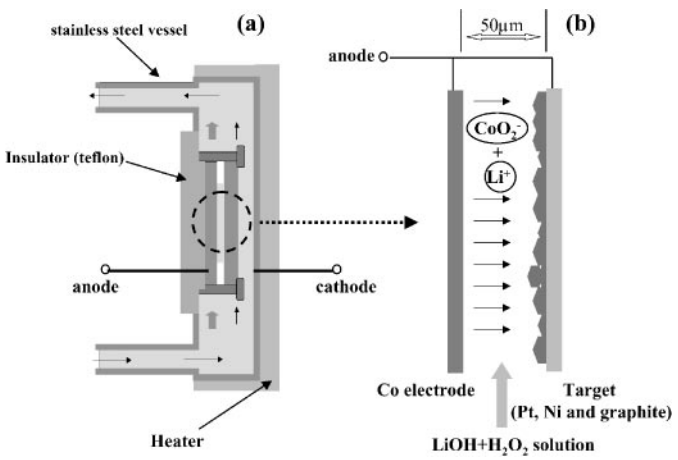

FIG. 2. Schematics of electrodes in the flow cell for hydrothermal–electrochemical reactions (a); dual- anode unit of Co and target (Pt, Ni) electrode (b).

the formation and microstructural control of $LiCoO_2$ films are reported in another paper (26). Similar treatment with cobalt and target metal electrodes in the dual anode system led to the formation of apparent black films on the target electrode (Pt, Ni, and graphite).

The surface morphology, crystal phase, crystallinity, and phase purity of prepared films were subsequently confirmed by SEM observation, X-ray diffraction (XRD) analysis, and Raman scattering spectroscopy, respectively. The SEM cross-sectional view of the prepared film (Fig. 3) directly confirms film formation on the platinum substrate with thickness of about 5 μm. As shown in Fig. 4, the surface morphology of fabricated films on the platinum substrate was obviously changed by the fabrication temperatures. It is clear from those pictures that grain size initially increases and then decreases with increasing temperature. At 150°C, the $LiCoO_2$ crystals showed a maximum size of about 2–3 μm in diameter. The $LiCoO_2$ film has also been fabricated on an Ni substrate using the same conditions at 150°C. The formed film consists of hexagonal-plate-shaped $LiCoO_2$ crystals, a few μm in diameter (Fig. 5). The XRD patterns of fabricated films on platinum substrates with various temperatures are shown in Fig. 6. The presence of the peak near 19° (003) in the XRD patterns directly indicates the formation of polycrystalline $LiCoO_2$ film on the substrate. The film fabricated at 150°C seems to have higher thickness and/or crystallinity than the others because the XRD peaks are strongest. This also corresponds to the results of the SEM observations mentioned above. This

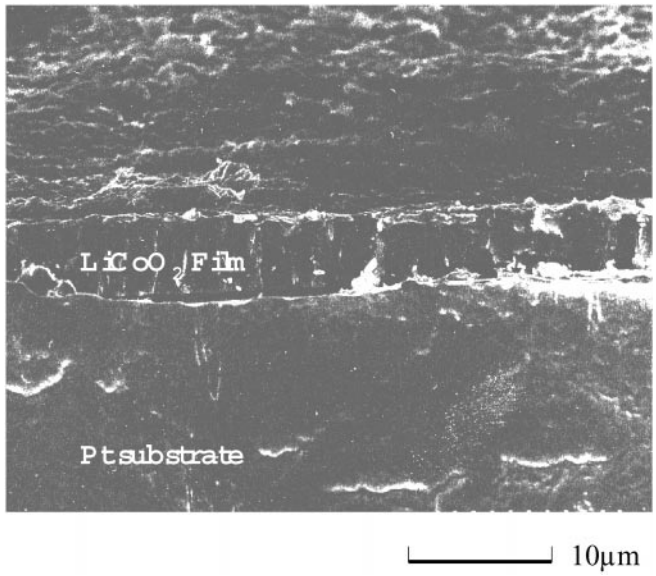

FIG. 3. The SEM cross-sectional view of the film on the platinum substrate prepared by hydrothermal–electrochemical methods at 150°C for 2 h.

phenomenon can be explained by the balance of nucleation rate, growth rate, and redissolution rate of crystals in the solution. Generally, both the growth rate and the solubility of the crystal increase with increasing temperature. Under our fabrication conditions below 150°C, for which the crystal grain size increases with increasing temperature, the

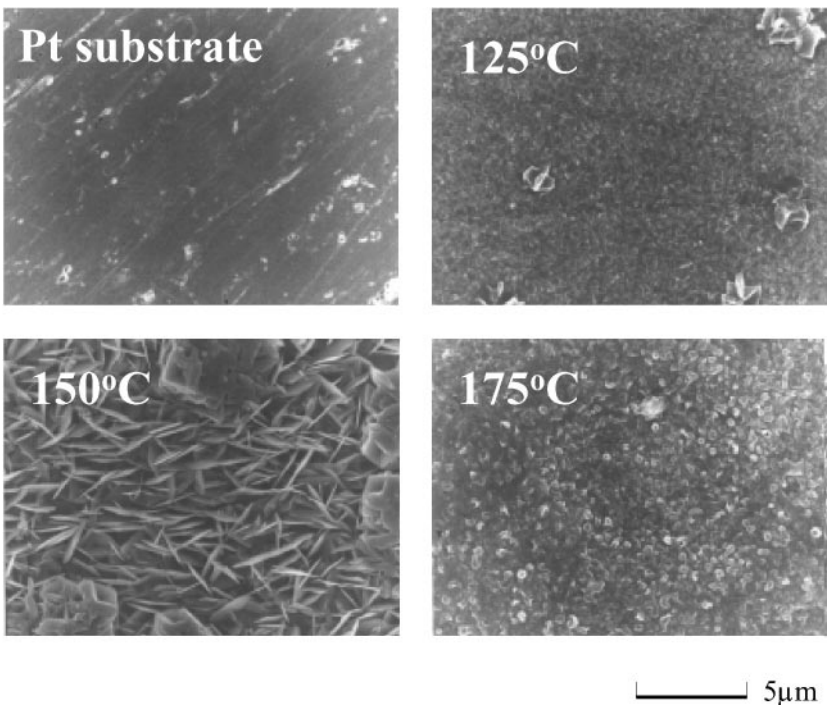

FIG. 4. The SEM images of the $LiCoO_2$ films fabricated on platinum substrate by hydrothermal–electrochemical methods at 125, 150, and 175°C for 2 h.

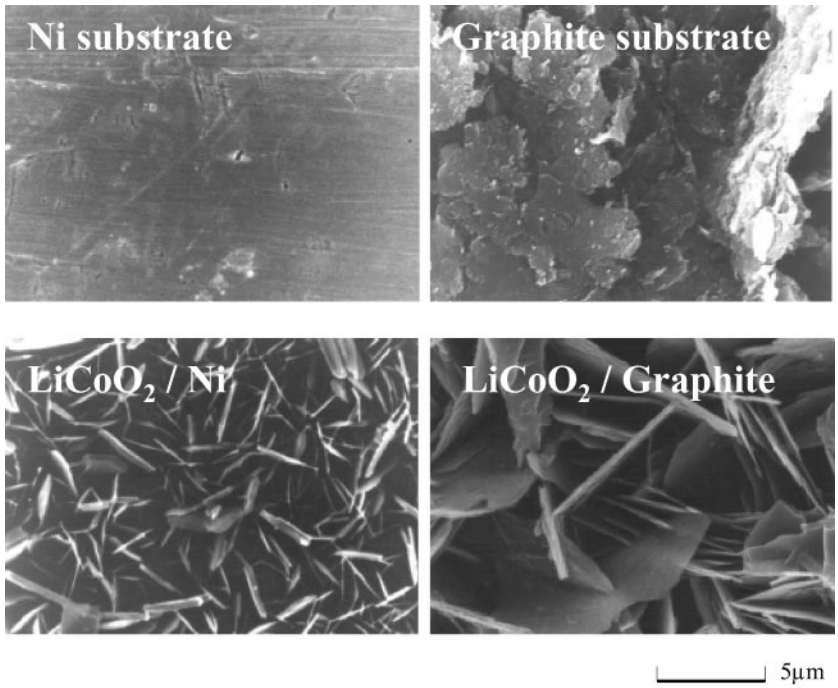

FIG. 5. The SEM images of the untreated nickel surface and the $LiCoO_2$ films fabricated on nickel substrate by hydrothermal–electrochemical methods at 150°C for 2 h.

growth rate seems to dominate over the nucleation rate. In other words, we can consider two temperature domains. In the first one, up to 150°C, the crystal growth rate increases with the temperature. Thus, well-crystallized $LiCoO_2$ can be formed around 150°C. In the second one, above 150°C, the increased redissolution rate of formed crystal probably dominates, leading to a decrease in the grain size of $LiCoO_2$ crystals with increasing temperature. An opposite phenomenon was observed in our previous study of temperature dependence of the $BaTiO_3$ film on titanium substrate (17). This difference can be explained by the solubilities of those crystals under certain conditions of hydrothermal solution. $BaTiO_3$ has less solubility in the operating conditions, thus its deposition on the other substrates is more difficult than that of $LiCoO_2$. The present study also shows that fabrication temperature may allow the phase control in the films.

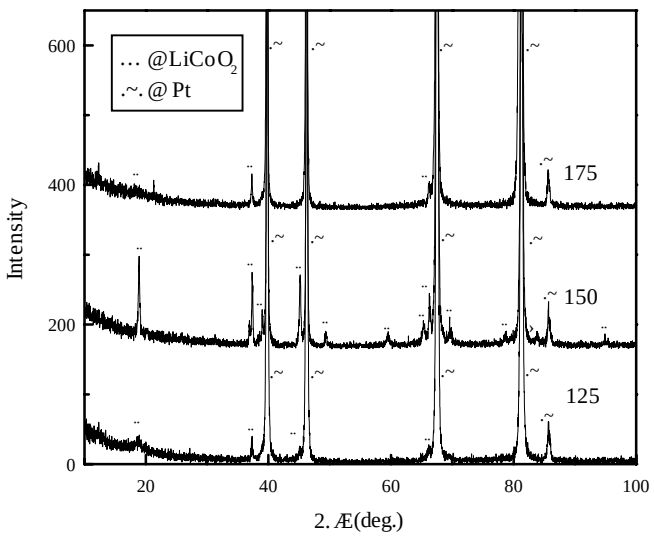

FIG. 6. X-ray diffraction patterns of $LiCoO_2$ films fabricated on platinum substrate by hydrothermal–electrochemical methods at 125, 150, and 175°C for 2 h.

It is widely known that $LiCoO_2$ has three structural phases, hexagonal with $R\bar{3}m$ space group, spinel with $Fd3m$ and cubic with $Fm3m$ (27–31). Among these, the spinel and hexagonal phases are well known to exhibit electrochemical activity. Generally, the spinel $Fd3m$ phase is synthesized around 400°C and the layered hexagonal one $R\bar{3}m$ is observed at higher temperatures (>800°C) (32, 33). However, identification of each phase is difficult using only XRD analysis because the XRD patterns of those phases are quite similar. Raman spectroscopy allows the distinction between different coordination sites, which produce different Raman active vibration modes. The group theoretical analysis based on their point groups predicts different vibration modes. The irreducible representations for optical vibration modes in layered hexagonal $LiCoO_2$ are $\Gamma_{\text{vib.}} = \Gamma(\text{Li}) + \Gamma(\text{Co}) + \Gamma(\text{O}) - \Gamma_{\text{trans.}} = A_{1g}(R) + E_g(R) + 2A_{2u}(\text{IR}) + 2E_u(\text{IR})$, where R and IR indicate Raman and IR active modes, respectively, predicting two Raman active modes

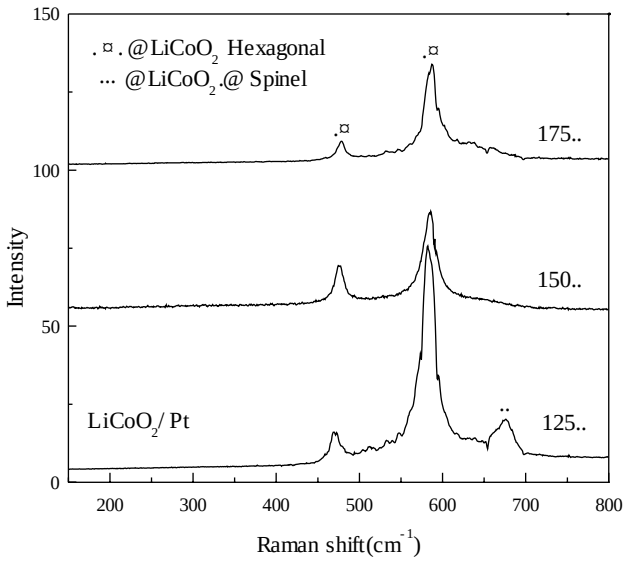

FIG. 7. Raman scattering spectra of $LiCoO_2$ films fabricated on platinum substrate by hydrothermal–electrochemical methods at 125, 150, and 175°C for 2 h.

(34–37). It has been noted that the Raman active A_{1g} and E_g modes do not originate from Li and Co; that is, only the oxygen atoms vibrate in these modes. On the other hand, the irreducible representations for cubic spinel-type $LiCoO_2$ are $\Gamma_{vib.} = \Gamma(Li) + \Gamma(Co) + \Gamma(O) - \Gamma_{trans.} = A_{1g}(R) + E_g(R) + F_{1g}(N) + 2F_{2g}(R) + 3A_{2u}(N) + 3E_u(N) + 5F_{1u}(IR) + 3F_{2u}(N)$, where N means that the vibrational modes are neither Raman nor IR active, resulting in four Raman active modes (34–37). Therefore, two A_{1g} and E_g modes are Raman active in layered $LiCoO_2$, which can be represented as $A_{1g} + E_g + 2A_{2u} + 2E_u$, but four A_{1g}, E_g, and $2F_{2g}$ modes are Raman active in the spinel $Li_{1-x}CoO_2$, which can be represented as $A_{1g} + E_g + 2F_{2g} + 5F_{1u}$ (37).

As shown in Fig. 7, two strong Raman modes at around 486 and 596 cm^{-1} are observed for prepared $LiCoO_2$ films with various temperatures on platinum substrates. The peak positions of Raman scattering agree exactly with those of the layered $LiCoO_2$ phase structure (35–37). No probable side products, such as Li_2CO_3 and $Co(OH)_2$, have been detected via Raman measurements. However, the Raman spectra of the films obtained at a temperature higher than 125°C seems to include small amounts of spinel-structured $Li_{1-x}CoO_2$ phase, scattered at around 690 cm^{-1}. The spinel phase is considered to have less electrochemical activity than the hexagonal one in the field of lithium ion battery electrodes. This therefore reveals the control of the $LiCoO_2$ structural phase in the film through fabrication temperature control. Raman spectra of the film fabricated on Ni substrate by using same operating conditions at 150°C also agree with the spectra of the $LiCoO_2$ hexagonal phase (Fig. 8).

Here we would like to propose the formation mechanism of $LiCoO_2$ film in the present study, which seems to be based on (a) dissolution, (b) oxidation, and (c) precipitation mechanisms as follows:

(a) Electrochemical oxidation and dissolution of Co anode:

$$Co + 3OH^- \rightarrow HCoO_2^- + H_2O + 2e^-, \text{ Co: } 0 \rightarrow 2^+ \quad [1]$$

(b) Oxidation in the solution:

$$2HCoO_2^- + H_2O_2 \rightarrow 2CoO_2^- + 2H_2O, \text{ Co: } 2^+ \rightarrow 3^+ \quad [2]$$

(c) Precipitation of $LiCoO_2$ on the target substrate (Pt, Ni):

$$CoO_2^- + Li^+ \rightarrow LiCoO_2. \quad [3]$$

According to the Pourbaix's diagram (38), $HCoO_2^-$ ions can be formed in the vicinity of the cobalt electrode in alkaline solution by anodic oxidation of the Co plate as described by Eq. (1). When the pH of the alkaline solution is not high enough, the subreaction can proceed to form cobalt hydroxide $Co(OH)_2$ as an impurity in the fabricated films. In the second reaction stage, formed $HCoO_2^-$ ion is oxidized from Co^{2+} to Co^{3+} by reaction with H_2O_2 in the solution (2). The CoO_2^- ion generated by this reaction can be delivered to the vicinity of the Co electrode of the target substrate. Thus it reacts with surrounding Li^+ ion in Eq. (3). As a result of this reaction, $LiCoO_2$ can nucleate both on

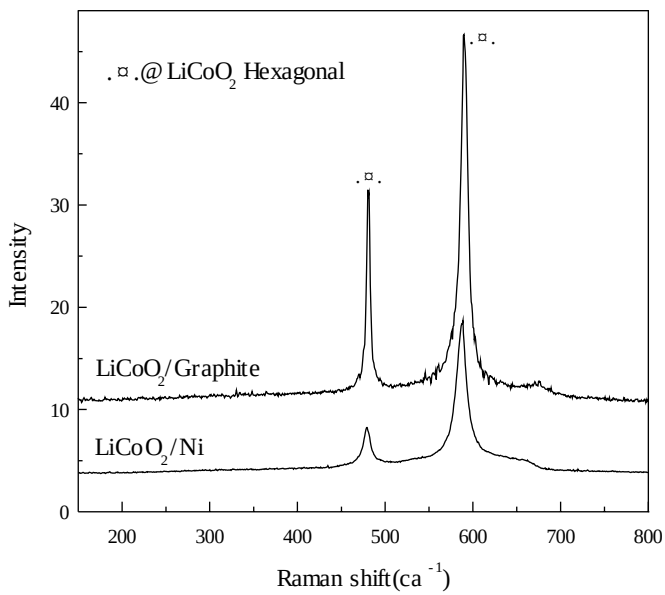

FIG. 8. Raman scattering spectra of $LiCoO_2$ films fabricated on nickel substrate by hydrothermal–electrochemical methods at 150°C for 2 h.

the Co and on the target substrates. It grows to form $LiCoO_2$ crystals, which might finally cover the substrates as a film. The driving force in the reaction of the dissolved cobalt species is the high concentration of Li^+ in the solution under hydrothermal conditions. The subsequent step is the heterogeneous nucleation and crystal growth of $LiCoO_2$ on the substrate surface to form a film under hydrothermal conditions; these processes could be further accelerated at a higher fabrication temperature. However, a fabrication temperature around 125°C seems to provide an insufficient driving force in this system to produce completely cation-ordered hexagonal $LiCoO_2$, resulting in the formation of a spinel phase where cation ordering is imperfect (39, 40). In general, cation ordering needs a higher activation energy than formation of the cation disordered phase, so that the formation reaction of the hexagonal $LiCoO_2$ phase is certainly more difficult than that for the spinel phase at a lower temperature. Increasing the fabrication temperature provides a higher activation energy to form hexagonal $LiCoO_2$. Therefore, of particular interest in our observations is the control of the phase selection of spinel or hexagonal $LiCoO_2$ during the hydrothermal processing.

CONCLUSIONS

We have clearly shown the usefulness of the hydrothermal–electrochemical process for the direct fabrication of $LiCoO_2$ films on Co, Pt, Ni, and graphite substrates at 100–175°C. Using a dual anode system with these target substrates, a well-crystallized $LiCoO_2$ phase has been directly deposited on the various substrates at low temperature by soft solution processing for the first time. In this research, we also succeeded in fabrication $LiCoO_2$ films in a shorter reaction time (2 h) by using our flow cell with continuously added H_2O_2 as an oxidant; that is, the oxidant in the solution played an important role in accelerating the oxidation reaction of Co^{2+} ion to Co^{3+} ion. The above results suggests that the formation of $LiCoO_2$ films under our hydrothermal conditions is based on the dissolution–oxidation–precipitation mechanism. The subsequent step is the heterogeneous nucleation and crystal growth of $LiCoO_2$ particles on the substrate. It is found that a fabrication temperature of 150°C is the most adequate for the formation of the $LiCoO_2$ hexagonal phase film under our experimental conditions.

ACKNOWLEDGMENTS

This research was supported by the "Research for the Future" Program 96R06901 of the Japanese Society for the Promotion of Science (JSPS). The author, T. Watanabe, was supported by a "Research Fellowships of the JSPS." The authors are greatly indebted to Professor M. Kakihana and to Dr. W. L. Suchanek, Dr. P. Krtil, Dr. T. Fujiwara, Mr. R. Teranishi, Mr. M. Endo, and Miss E. Orhan for stimulating discussions.

REFERENCES

1. F. K. Shokoohi, J. M. Tarascon, and B. J. Wilkens, *Appl. Phys. Lett.* **59,** 1260–1262 (1991).
2. F. K. Shokoohi, J. M. Tarascon, B. J. Wilkens, D. Guymard, and C. C. Chang, *J. Electrochem. Soc.* **139,** 1845–1849 (1992).
3. A. Antaya, J. R. Dahn, J. S. Preston, E. Rossen, and J. N. Reimers, *J. Electrochem. Soc.* **140,** 575–578 (1993).
4. K.-H. Hwang, S.-H. Lee, and S.-K. Joo, *J. Electrochem. Soc.* **141,** 3296–3299 (1994).
5. A. Antaya, K. Cearns, and J. S. Preston, *J. Appl. Phys.* **76,** 2799–2806 (1994).
6. S. J. Lee, J. K. Lee, D. W. Kim, and H. K. Baik, *J. Electrochem. Soc.* **143,** L268–270 (1996).
7. C. B. Wang, J. B. Bates, F. X. Hart, B. C. Sales, R. A. Zhur, and J. D. Robertson, *J. Electrochem. Soc.* **143,** 3203–3213 (1996).
8. K. A. Striebel, C. Z. Deng, S. J. Wen, and E. J. Cairns, *J. Electrochem. Soc.* **143,** 1821–1827 (1996).
9. M. Yoshimura, W. L. Suchanek, and K. Byrappa, *MRS Bull.* **25**(9), 17–25 (2000).
10. M. Yoshimura, *J. Mater. Res.* **13,** 796–802 (1998).
11. M. Yoshimura, S. E. Yoo, M. Hayashi, and N. Ishizawa, *Jpn. J. Appl. Phys.* **28,** L2007–2009 (1989).
12. Kajiyoshi, K. Tomono, Y. Hamaji, T. Kasanami, and M. Yoshimura, *J. Am. Ceram. Soc.* **77,** 2889–2897 (1994).
13. Y. G. Gogotsi and M. Yoshimura, *Nature* **367,** 628–630 (1994).
14. W. S. Cho, M. Yashima, M. Kakihana, A. Kudo, T. Sakata, and M. Yoshimura, *Appl. Phys. Lett.* **66,** 1027–1029 (1995).
15. K. Kajiyoshi and M. Yoshimura, *Eur. J. Solid State Inorg. Chem.* **33,** 623–635 (1996).
16. W. S. Cho and M. Yoshimura, *J. Am. Ceram. Soc.* **80,** 2199–2204 (1997).
17. W. Suchanek, T. Watanabe, and M. Yoshimura, *Solid State Ionics* **109,** 65–72 (1998).
18. Tomoaki Watanabe, Woo-Seok Cho, Wojciech L. Suchanek, Masakazu Endo, Yasuro Ikuma, and Masahiro Yoshimura, *Solid State Sci.* **3,** 183–188 (2001).
19. M. Yoshimura, K. S. Han, and S. Tsurimoto, *Solid State Ionics* **106,** 39–44 (1998).
20. K. S. Han, S. W. Song, and M. Yoshimura, *Chem. Mater.* **10,** 2183–2188 (1998).
21. K. S. Han, P. Krtil, and M. Yoshimura, *J. Mater. Chem.* **8,** 2043–2048 (1998).
22. K. S. Han, S. W. Song, T. Watanabe, and M. Yoshimura, *Electrochem. Solid State Letters* **2**(2), 63–66 (1999).
23. S. W. Song, K. S. Han, I. Sasagawa, T. Watanabe, and M. Yoshimura, *Solid State Ionics* **135,** 277–281 (2000).
24. K. S. Han, S. W. Song, and M. Yoshimura, *J. Am. Ceram. Soc.* **81,** 2465–2468 (1998).
25. Wojciech L. Suchanek, Tomoaki Watanabe, Bungo Sakurai, Naoki Kumagai, and M. Yoshimura, *Rev. Sci. Instrum.* **70**(5), 2432–2437 (1999).
26. T. Watanabe, H. Uono, S.-W. Song, K. S. Han, and M. Yoshimura, submitted for publication.
27. K. Mizushima, P. C. Jones, P. J. Wiseman, and J. B. Goodenough, *Mater. Res. Bull.* **15,** 783–789 (1980).
28. T. Ohzuku and A. Ueda, *J. Electrochem. Soc.* **141,** 2972–2977 (1994).
29. T. Nagaura, *in* "Proc. 5th International Seminar on Lithium Battery Technology and Applications, Deerfield Beach, FL, 1990," pp. 5–7.
30. E. Zhecheva, R. Stoyanova, J. Gorova, R. Alcantara, J. Morales, and J. L. Tirado, *Chem. Mater.* **8,** 1429–1440 (1996).
31. B. Garicia, J. Farcy, J. P. Pereira-Ramos, and N. Baffier, *J. Electrochem. Soc.* **144,** 1179–1184 (1997).
32. R. J. Gummow, D. C. Liles, and M. M. Thackeray, *Mater. Res. Bull.* **28,** 235–246 (1993).

33. T. Ohzuku and A. Ueda, *J. Electrochem. Soc.* **141,** 2972–2977 (1994).
34. W. Huang and R. Frech, *Solid State Ionics* **86–88,** 395–400 (1996).
35. M. Inaba, Y. Todzuka, H. Yoshida, Y. Grincourt, A. Tasaka, Y. Tomida, and Z. Ogumi, *Chem. Lett*. 889–890 (1995).
36. M. Inaba, Y. Iriyama, Z. Ogumi, Y. Todzuka, and A. Tasaka, *J. Raman. Spectrosc.* **28,** 613–617 (1997).
37. W. G. Fately, "Infrared and Raman Selection Rules for Molecular and Lattice Vibrations," Wiley-Interscience, New York, 1972.
38. M. Pourbaix, "Atlas of Electrochemical Equilibria in Aqueous Solutions," translated by J. A. Franklin. National Association of Corrosion Engineers, Houston, 1974.
39. C. Wolverton and A. Zunger, *Phys. Rev. B* **57,** 2242–2252 (1998).
40. C. Wolverton and A. Zunger, *J. Electrochem. Soc.* **145,** 2424–2430 (1998).